Title
Reversal-field memory in the hysteresis of spin glasses.

Permalink
https://escholarship.org/uc/item/76m143v8

Journal
Physical review letters, 89(25)

ISSN
0031-9007

Authors
Katzgraber, H G
Pázmándi, F
Pike, C R
et al.

Publication Date
2002-12-16

DOI
10.1103/PhysRevLett.89.257202

Peer reviewed

Reversal-Field Memory in the Hysteresis of Spin Glasses

H. G. Katzgraber,[1] F. Pázmándi,[1] C. R. Pike,[2] Kai Liu,[1] R. T. Scalettar,[1] K. L. Verosub,[2] and G. T. Zimányi[1]

[1]*Department of Physics, University of California, Davis, California 95616*
[2]*Department of Geology, University of California, Davis, California 95616*

We report a novel singularity in the hysteresis of spin glasses, the reversal-field memory effect, which creates a nonanalyticity in the magnetization curves at a particular point related to the history of the sample. The origin of the effect is due to the existence of a macroscopic number of "symmetric clusters" of spins associated with a local spin-reversal symmetry of the Hamiltonian. We use first order reversal curve (FORC) diagrams to characterize the effect and compare to experimental results on thin magnetic films. We contrast our results on spin glasses to random magnets and show that the FORC technique is an effective "magnetic fingerprinting" tool.

The nonequilibrium behavior of random magnets and spin glasses is an intensely studied field, posing formidable theoretical and experimental challenges directly for magnetic systems, and also serving as paradigms for other fields. Concepts developed for random magnets such as glassy phases, droplet and replica theories, as well as aging have subsequently been applied to fields as diverse as structural biology, geology, and even financial analysis.

The slow and complex time dependence of various correlators is a hallmark of such systems. Several aspects of this nonequilibrium dynamics have already been described in great detail for spin glasses [1]. Hysteresis is one of the most central of these phenomena [2], yet while many basic features are qualitatively understood [3–5], theoretical descriptions of hysteresis even in the simplest spin-glass models are in their early stages [6]. Hysteresis in magnetic systems has a host of practical applications including magnetic recording and sensors, but a less than complete understanding at a fundamental level [2].

In this paper, we present a detailed study of several new aspects of hysteresis in two of the most commonly studied models of disordered magnets. One is the random-field Ising model (RFIM), which has been shown to describe successfully many of the relevant aspects of hysteresis [3]. The second is the Edwards-Anderson Ising spin glass (EASG), which, unlike the RFIM, contains frustration, a phenomenon known to introduce a whole new level of complexity in disordered systems. Accordingly, we show that the hysteretic properties of the EASG can be significantly different from those of the RFIM.

Our first important observation is of a novel memory effect in the hysteresis of the EASG that emerges when the magnetic field is first decreased from its saturation value and then increased again from some reversal-field H_R. We find that the EASG exhibits a singularity at the negative of the reversal field, $-H_R$, in the form of a kink in the magnetization of the reversal curve. By calculating a suitable overlap function, we demonstrate that the microscopic origin of the effect is due to a macroscopic number of symmetric clusters. In these clusters the central spins flip *after* all spins on the cluster surface have flipped. Therefore, the central spins experience an effective local field which is symmetric with respect to the change of direction of the external field.

This reversal-field memory effect can be even more precisely characterized with the recently introduced first order reversal curve (FORC) method [7]. As we shall demonstrate, the FORC technique provides a uniquely sensitive characterization of hysteretic systems and specifically of the difference between the hysteretic behavior of the RFIM and the EASG. The sharp kink of the minor loops of the EASG is captured as a profound horizontal ridge in FORC diagrams, indicative of a broad range of effective coercivities in the system, but a rather narrow range of biases. In contrast, despite exhibiting a major hysteresis loop rather similar to that of the EASG, the RFIM shows a strikingly different FORC diagram, characterized by a well-developed vertical feature reflecting a rather narrow range of effective coercivities and a broad range of biases.

Finally, we determine experimentally the reversal curves and FORC diagram of a magnetic thin film. Experimentally, the reversal curves show only smoothed kinks around $-H_R$. However, the FORC diagram of the data reveals a profound horizontal ridge, signaling the presence of a reversal-field memory in these films. This experimental result further highlights the usefulness of the FORC technique as a powerful method which captures the detailed behavior of hysteretic systems.

The Hamiltonian of the EASG is given by [8]

$$\mathcal{H} = \sum_{\langle i,j \rangle} J_{ij} S_i S_j - H \sum_i S_i. \tag{1}$$

Here $S_i = \pm 1$ are Ising spins on a square lattice of size $N = L \times L$ in two dimensions with periodic boundary conditions. The exchange couplings J_{ij} are random nearest-neighbor interactions chosen according to a

Gaussian distribution with zero mean and standard deviation unity, and H is the external magnetic field. We simulate the zero temperature dynamics of the EASG by changing the external field H in small steps, first downward from positive saturation and then upward from a reversal-field H_R. After each field step, the effective local field h_i of each spin S_i is calculated:

$$h_i = \sum_j J_{ij} S_j - H. \quad (2)$$

A spin is unstable if $h_i S_i < 0$. We then flip a randomly chosen unstable spin and update the local fields at neighboring sites and repeat this procedure until all spins are stable.

Figure 1 (solid line) shows the average of 10^3 reversal curves, all with the same H_R, but different disorder realizations. The area around $-H_R$ is enlarged in the inset and shows a "kink." The presence of any such sharp feature in a disordered system, especially of finite size and after disorder averaging, is quite remarkable.

The change of slope at the kink can be characterized by measuring the slope of the magnetization curves to the left and right of $-H_R$, and comparing the difference $\Delta(dM/dH)$ with the average $(dM/dH)_{ave}$ (see Fig. 2). The slope changes abruptly by as much as 30% as the field $H = -H_R$ is passed, creating the kink. With our parameters the kink is present in the range of reversal-field values $-4.0 < H_R < -1.5$.

In an effort to understand the microscopic origin of reversal-field memory, we first describe this effect within a phenomenological approach to hysteretic systems, the Preisach model [9]. In the Preisach model a magnetic system is described as a collection of independent two-state (± 1) switching units, or "hysterons." Unlike Ising spins, which always align with their local field, the hysteron's state changes from -1 to $+1$ at a field $H_b + H_c$, different from the field $H_b - H_c$, required to switch the hysteron from $+1$ to -1. Different systems are distinguished by their different distributions $\rho(H_b, H_c)$ of hysterons of a given bias H_b and coercivity H_c. Here $\rho(H_b, H_c)$ is the so-called "Preisach function."

An intuitive picture can be obtained by first considering symmetric hysterons, having no bias, i.e., $H_b = 0$. Starting from a fully "up" polarized state and decreasing the field to a negative H_R switches down all symmetric hysterons with $H_c < |H_R|$. Reversing the direction of the sweep and increasing the field from H_R to $-H_R$ along a reversal curve switches back every switched hysteron. Thus at $H = -H_R$ saturation is reached, creating a kink in the magnetization. Symmetric hysterons therefore give rise to reversal-field memory. However, this memory effect will be detectable only if the number of symmetric hysterons is macroscopic. This happens if $\rho(H_b, H_c)$ has a Dirac delta singularity at $H_b = 0$ and $H_c = |H_R|$. As the kink is observed in a range of H_R values, the singularities of the Preisach function form a horizontal ridge along the $H_b = 0$ axis for the corresponding range of $H_c = |H_R|$ values.

Next we move beyond phenomenological approaches, but keep the insight gained from the Preisach model. We carry over the concept of symmetric hysterons as symmetric clusters of the strongly interacting spins of the EASG. A spin S_i belongs to a symmetric cluster if S_i flips down only after all its neighbors have flipped down, and during the reverse sweep S_i flips up again only after all its neighbors have. Therefore, this central spin S_i experiences an effective local field which is symmetric with respect to the change of direction of the external field, in analogy to a symmetric hysteron.

Spins possessing *local spin-reversal symmetry* are candidates for symmetric hysterons. By local spin-reversal symmetry we mean that the local field h_i, felt by S_i [Eq. (2)], is perfectly reversed if the external field H is reversed and all spins coupled to S_i are reversed as well.
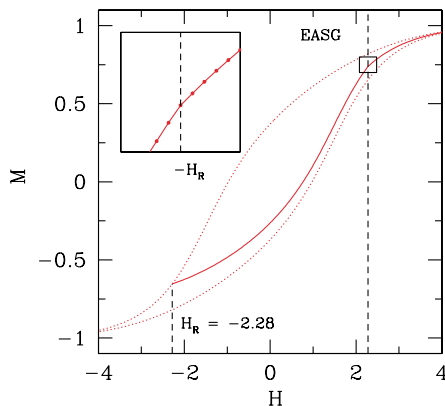

FIG. 1 (color online). Reversal curve (solid line) and major hysteresis loop (dotted line) for a two-dimensional (2D) EASG with 10^4 spins and $H_R = -2.28$. In the inset a kink is seen around $-H_R$. In all figures the error bars are smaller than the symbols.
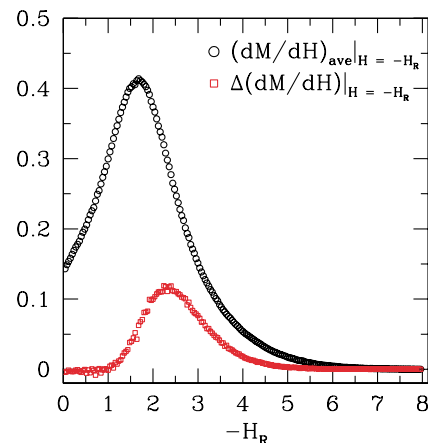

FIG. 2 (color online). The difference (squares) and average (circles) of the left and right derivatives at $-H_R$ for the EASG.

Every spin of the EASG has local spin-reversal symmetry. However, in a glassy system the spin configurations depend on the history of the sample. Therefore, at $-H_R$ the neighbors of most spins *do not necessarily point in a direction opposite their direction at H_R*, and thus most EASG spins do not belong to symmetric clusters. Hence the model Hamiltonian possessing a local spin-reversal symmetry is a necessary but not sufficient condition for having symmetric clusters.

To see a macroscopic kink it has to be shown that the density of symmetric clusters is finite. A lower bound on their density is obtained by considering the simplest symmetric cluster: two strongly coupled spins, weakly coupled to their six neighbors in a 2D lattice. The switching field of each spin is determined by these couplings. The outer spins will switch before the inner spins if their couplings are restricted by appropriate inequalities, confining the couplings to finite intervals. The density of symmetric clusters is obtained by integrating the product of the distributions of the couplings over these finite intervals. With unbounded coupling distributions, e.g., Gaussian, the product of the distributions is finite over the finite integration intervals, thus the resulting density is finite as well.

As a further evidence for the macroscopic number of symmetric clusters, we define an overlap function q between the spins which flip at H_R and the spins which flip at $H > H_R$:

$$q(H) = \frac{1}{4} \sum_i [S_i(H_R + \delta) - S_i(H_R)]$$
$$\times [S_i(H + \delta) - S_i(H)]. \qquad (3)$$

Here δ is the field step. In Fig. 3 we show the overlap $q(H)$ for $H_R = -2.28$. The large peak at $H = +2.28$ indicates that a macroscopic number of spins which have flipped at H_R, also flip at $-H_R$. This in turn means that there is a macroscopic number of symmetric clusters. The insets
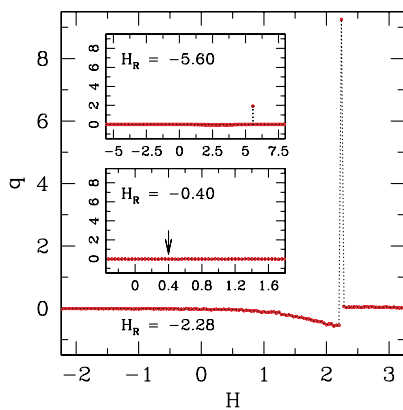
show a much smaller number of symmetric clusters at $H_R = -0.40$ and $H_R = -5.60$, values outside the peak of Fig. 2.

To characterize reversal-field memory further, we adapt a new tool developed for analyzing experimental data of hysteretic systems [7]. A family of FORCs with different H_R is generated, with $M(H, H_R)$ denoting the resulting magnetization as a function of the applied and reversal fields. Computing the mixed second order derivative $\rho(H, H_R) = -(1/2)[\partial^2 M / \partial H \partial H_R]$ and changing variables to $H_c = (H - H_R)/2$ and $H_b = (H + H_R)/2$, the local coercivity and bias, respectively, yield the "FORC distribution" $\rho(H_b, H_c)$. For phenomenological Preisach models, the FORC distribution is equal to the Preisach function. However, FORC distributions are more general, because they are extracted from numerical or experimental data, and thus are model independent.

Figure 4 shows the FORC diagram of the EASG. The ridge along the H_c axis in the range $1.5 < H_c < 4.0$ corresponds to the ridge of Fig. 2, representing the kinks of Fig. 1. Thus FORC diagrams capture the reversal-field memory effect in the form of a ridge along the H_c axis.

To demonstrate that local spin-reversal symmetry of the Hamiltonian is necessary for reversal-field memory to be present, we study the RFIM [3,8]. In this model $J_{ij} = 1$ and the disorder is introduced through random local fields chosen according to a Gaussian distribution with zero mean and standard deviation Δ. Direct inspection reveals that the RFIM *does not possess* a local spin-reversal symmetry. Therefore, the RFIM cannot have symmetric clusters and should not exhibit a reversal-field memory. This is confirmed by our simulations: a typical RFIM reversal curve shown in the right panel of Fig. 5 has no kink at $-H_R$.

Not only do the two models differ in the local spin symmetry, the EASG possesses frustration which might give rise to hysteretic phenomena that are qualitatively rather different than in the RFIM. To explore this possibility, we show in the left panel of Fig. 5 the FORC diagram for the RFIM for a disorder $\Delta = 4.0$. While the major hysteresis loop of the RFIM is very similar to that of the EASG, the FORC distribution is qualitatively different: it exhibits a predominantly vertical feature. The distribution of random fields of the RFIM introduces a
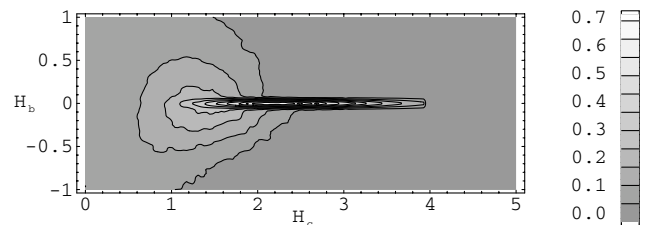

FIG. 3 (color online).   Overlap function q of the spins flipping at H_R and at $H > H_R$, for $H_R = -2.28$. The insets show data for $H_R = -0.40$ and $H_R = -5.60$. The arrow in the inset marks $H = 0.40$.

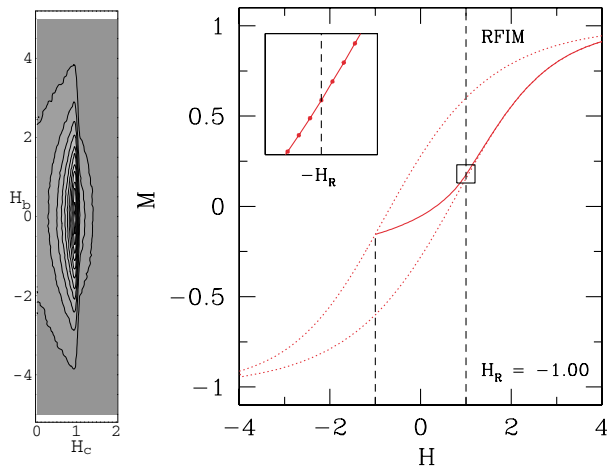FIG. 4.   FORC Diagram of the EASG. Note the ridge along the H_c axis.

FIG. 5 (color online).   FORC Diagram of the 2D RFIM. Data for $\Delta = 4.0$, $N = 10^4$ spins and 10^3 disorder realizations (same scale as in Fig. 4). Note the clear differences to the FORC diagram of the EASG (Fig. 4). The right panel shows the major hysteresis loop (dotted line) and a reversal curve (solid line) for $H_R = -1$. The inset shows an enlarged view of the region around $-H_R$.

FIG. 6.   Experimental FORC diagram of a Kodak sample. Note the similarity to the FORC diagram of the EASG shown in Fig. 4.

large range of biases for the spins, with little variation in the local coercivity. This expectation is confirmed by simulations of the RFIM with various disorder distributions, which show that the vertical cross section of the vertical feature mirrors the shape of the random field distribution.

Finally, we demonstrate the existence of reversal-field memory in experimental systems. We study thin films of well-dispersed single-domain magnetic Co-γ-Fe$_2$O$_3$ particles provided by Kodak, Inc. We determine both the individual reversal curves and the FORC diagram of the system. While the reversal-field memory kinks in $-H_R$ are somewhat smoothed, the FORC diagram clearly exhibits the horizontal ridge associated with the reversal-field memory effect (Fig. 6). This striking similarity between the experimentally determined FORC diagram of the Co-γ-Fe$_2$O$_3$ films and the numerically determined FORC diagram of the EASG indicates not only that Co-γ-Fe$_2$O$_3$ films exhibit reversal-field memory but also that frustration may be a component of the physics of the Co-γ-Fe$_2$O$_3$ films.

In conclusion, we have reported a novel reversal-field memory effect in the EASG that manifests itself as a sharp kink in first order reversal curves and also as a sharp ridge on the zero bias axis of FORC diagrams. We suggest the microscopic origin of the effect is the presence of a macroscopic number of "symmetric clusters," and prove this by computing a suitable overlap function. We further show that reversal-field memory is absent from the RFIM, which does not exhibit symmetric clus-
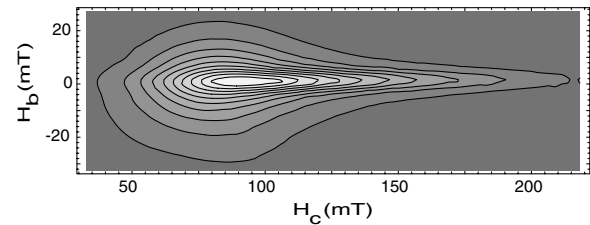
ters. While the hysteresis loops of the EASG and the RFIM are remarkably similar for corresponding parameters, their FORC diagrams are profoundly different, establishing that the FORC method is a powerful diagnostic tool for capturing the sensitive details of hysteretic systems such as spin glasses and random magnets. The FORC diagrams of several magnetic thin films exhibit a profound ridge indicative of the reversal-field memory effect in experimental systems. Simulations on more realistic magnetic models which include dipolar interactions have also shown the reversal-field memory effect. This suggests that the reversal-field memory is not specific to the EASG, but is a robust result for a large class of theoretical models and experimental systems.

[1] *Spin Glasses and Random Fields*, edited by A. P. Young (World Scientific, Singapore, 1998).
[2] G. Bertotti, *Hysteresis and Magnetism for Physicists, Materials Scientists, and Engineers* (Academic Press, New York, 1998).
[3] J. P. Sethna, K. Dahmen, S. Kartha, J. A. Krumhansl, B. W. Roberts, and J. D. Shore, Phys. Rev. Lett. **70**, 3347 (1993).
[4] I. F. Lyuksyutov, T. Nattermann, and V. Pokrovsky, Phys. Rev. B **59**, 4260 (1999).
[5] J. Zhu, in *Magnetic Recording Technology*, edited by C. D. Mee and E. D. Daniel (McGraw-Hill, New York, 1990).
[6] F. Pázmándi, G. Zaránd, and G. T. Zimányi, Phys. Rev. Lett. **83**, 1034 (1999).
[7] C. R. Pike, A. P. Roberts, and K. L. Verosub, J. Appl. Phys. **85**, 6660 (1999).
[8] K. Binder and A. P. Young, Rev. Mod. Phys. **58**, 801 (1986).
[9] F. Preisach, Z. Phys. **94**, 277 (1935).